

Characterisation of a Ruthenium Bipyridyl Dye Showing a Long-lived Charge-separated State on TiO₂ in the Presence of I⁻/I₃⁻

Keri L. McCall,^a Ana Morandeira,^b James Durrant^b Lesley J. Yellowlees^a and Neil Robertson^{*a}

Supplementary Information

Electrochemistry

TTF can undergo two reversible oxidations, yielding a stable radical cation and di-cation respectively. The electrochemistry of TTF and derivatives thereof are also known to be solvent-dependent.¹ This variation of oxidation potentials with solvent is thought to be due to solvents with a higher donor number being able to stabilise the dication more readily. (The donor number of a solvent is defined as the negative of the enthalpy of reaction between the solvent and antimony pentachloride.²) This effect was observed in the electrochemical study of $(\text{SC}_2\text{H}_4\text{CN})_2\text{TTF}(\text{SMe})_2$ (Fig. S1), with the difference between oxidation potentials (ΔE) being smaller in DMF ($\Delta E = 0.14$ V), a solvent with a donor number of 26.6 kcal/mol, relative to DCM ($\Delta E = 0.26$ V) which has a negligible donor number.

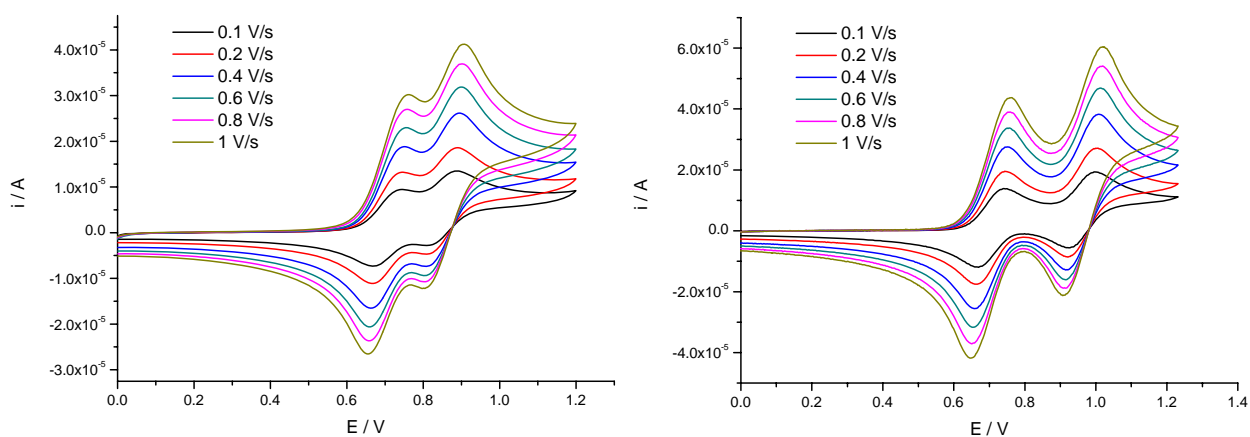


Figure S1. CV studies of $(\text{SC}_2\text{H}_4\text{CN})_2\text{TTF}(\text{SMe})_2$ in 0.1 M TBABF₄/DMF (left) and 0.3 M TBABF₄/DCM (right).

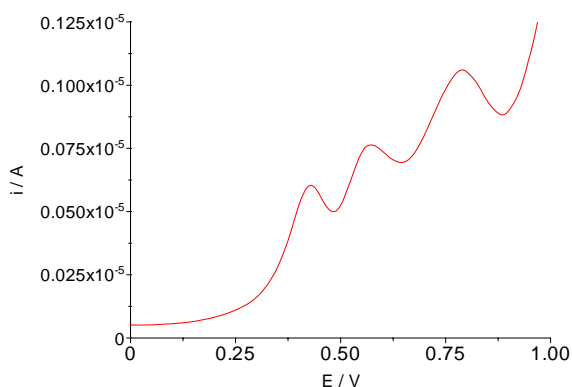


Figure S2. Differential pulse study of **1** in 0.1 M TBABF₄/DMF.

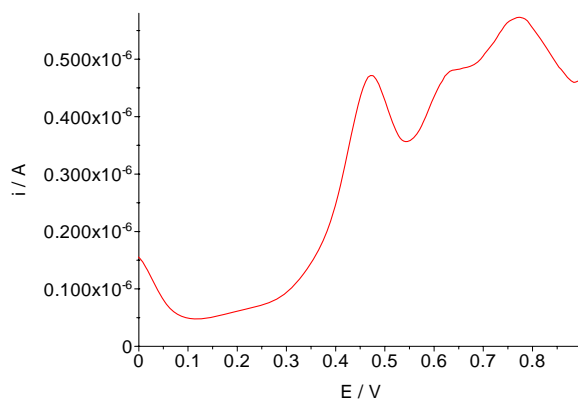


Figure S3. Differential pulse study of **2** in 0.1 M TBABF₄/DMF.

Absorption spectroscopy

(SC₂H₄CN)₂TTF(SMe)₂ shows a number of strong UV transitions and a weak band in the visible region, resulting in a yellow/orange solution.

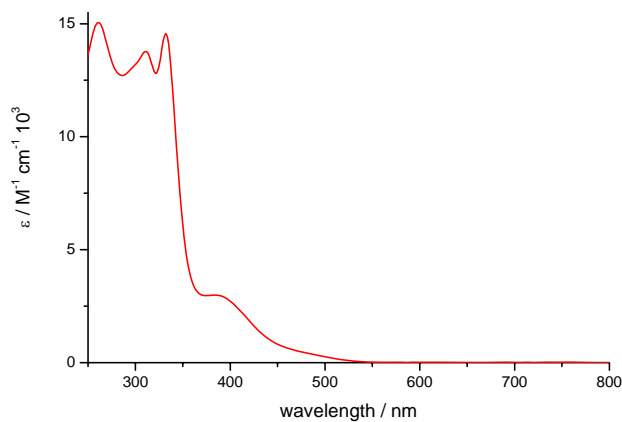


Figure S4. Absorption spectrum of (SC₂H₄CN)₂TTF(SMe)₂ in DCM.

Emission Studies

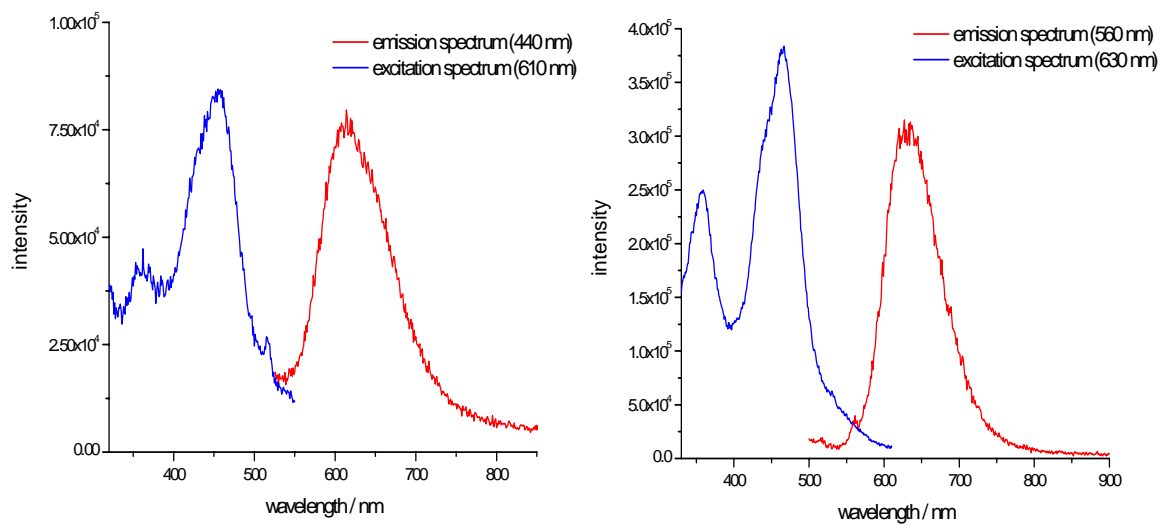


Figure S5. Excitation and emission spectra of **1** (left) and **2** (right) in ethanol at room temperature, with corresponding excitation and emission wavelengths shown in brackets.

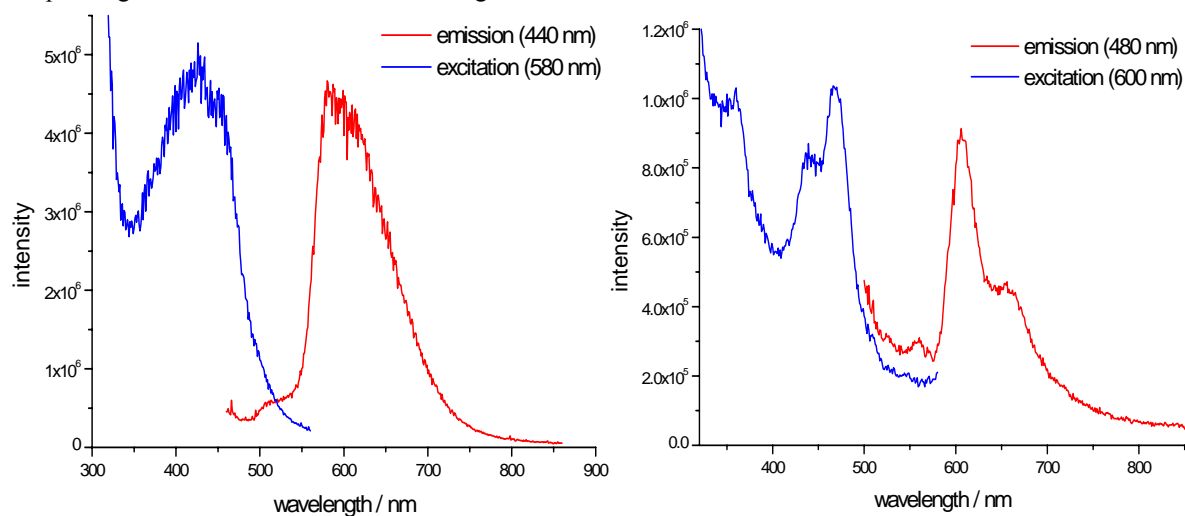


Figure S6. Excitation and emission spectra of **1** (left) and **2** (right) in rigid glass at 77 K, with corresponding excitation and emission wavelengths shown in brackets.

Spectroelectrochemistry

OTTLE

The OTTLE studies of $(\text{SC}_2\text{H}_4\text{CN})_2\text{TTF}(\text{SMe})_2$ in 0.3 M TBABF₄/DCM showed very clear changes to the absorption spectra for the mono-oxidised and di-oxidised species (Table S1, Fig. S7). The first oxidation results in the growth of visible region bands at 22000 and 12000 cm^{-1} and the complete collapse of two of the UV bands as well as the decrease in intensity of the third UV band. The second oxidation results in the collapse of the two visible region bands and the growth of a more intense band at 14800 cm^{-1} . Two new bands were also observed in the UV region at 42600 and 34000 cm^{-1} . The two bands in the visible region for the mono-oxidised species must involve the resultant singly-occupied molecular orbital (SOMO) as they consequently collapse upon di-oxidation. It is likely that these transitions are intramolecular SOMO to lower unoccupied orbitals and/or HOMO-1 to SOMO. It should be noted that these studies were also carried out in 0.1 M TBABF₄/DMF and showed irreversible behaviour with no isosbestic points during the oxidised species generation, suggesting degradation of the oxidised species in this more coordinating solvent.

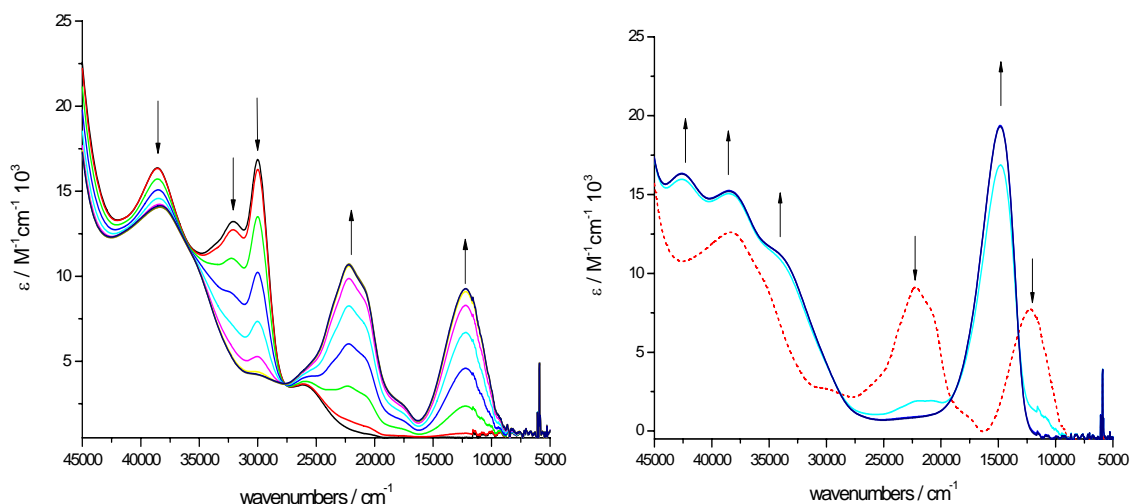


Figure S7. Oxidative OTTLE study of $(\text{SC}_2\text{H}_4\text{CN})_2\text{TTF}(\text{SMe})_2$ showing mono-oxidation (left) and di-oxidation (right) in 0.3 M TBABF₄/DCM, at -40 °C with applied potentials of + 0.85 and + 1.25 V respectively (vs. Ag/AgCl). Mono-oxidised spectrum is shown as a dashed line in right hand graph for clarity.

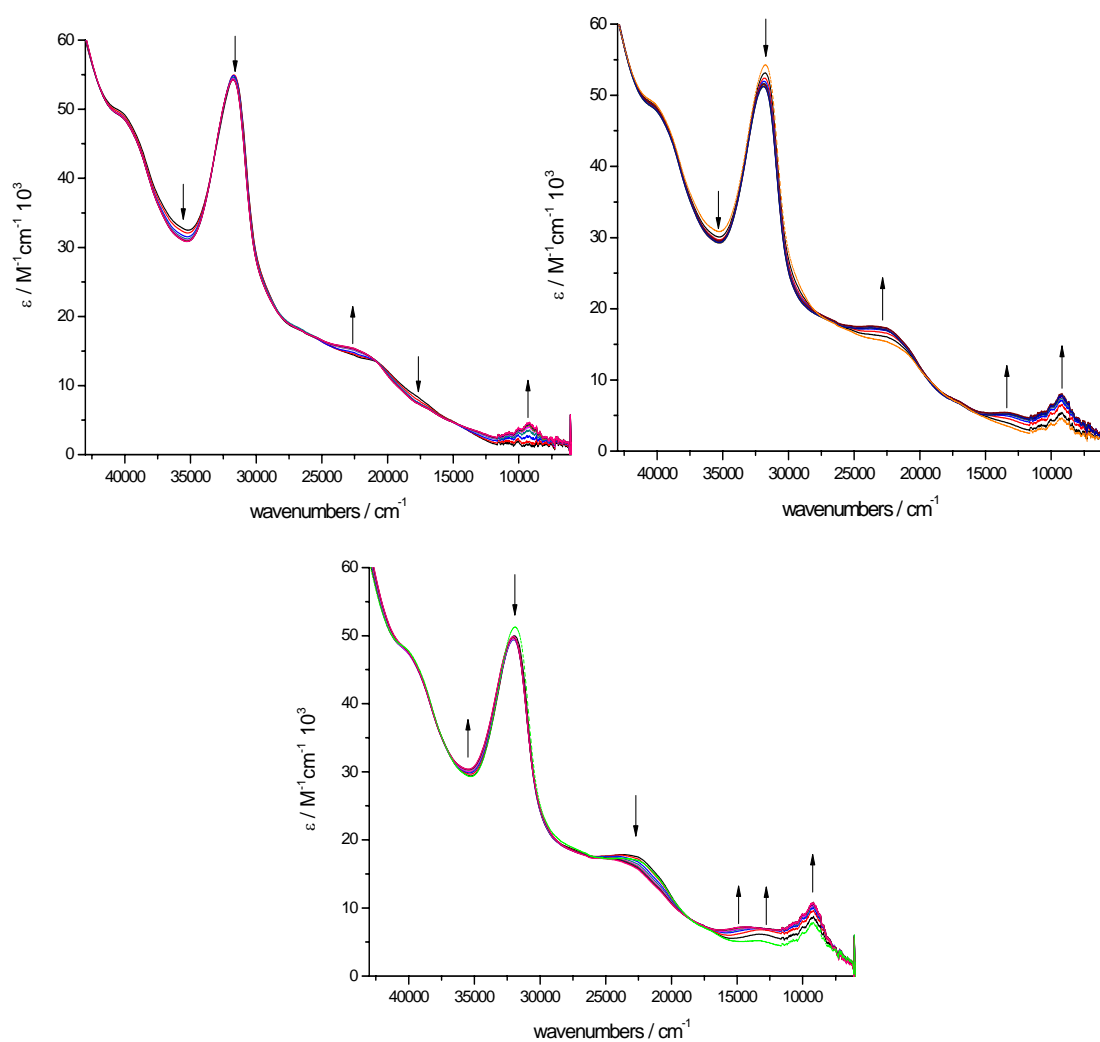


Figure S8. Oxidative OTTLE studies of **2** in 0.3 M TBABF₄/DCM, showing mono-oxidised (top left), di-oxidised (top right) and tri-oxidised (bottom), with applied potentials of + 0.5, + 0.68 and + 0.91 V respectively (vs. Ag/AgCl).

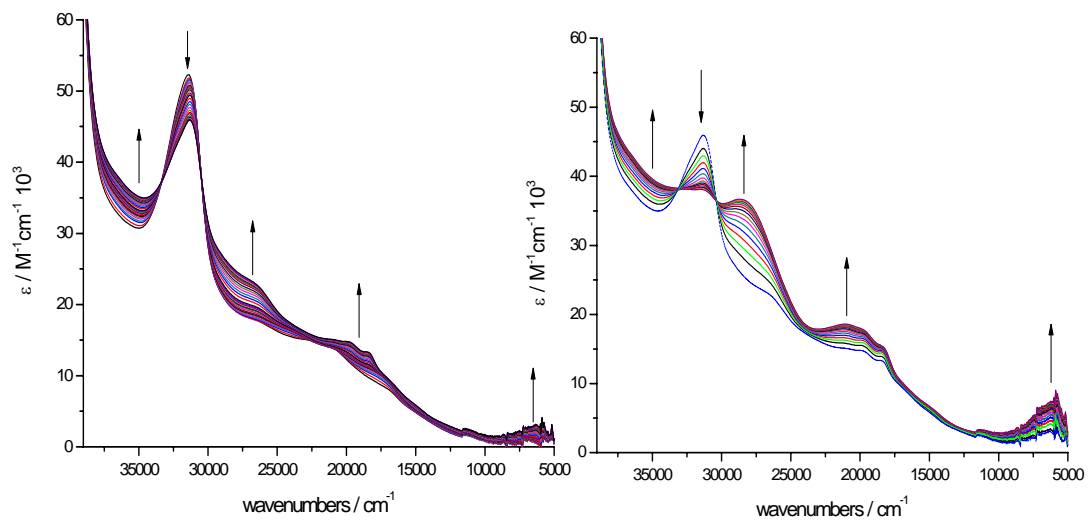


Figure S9. Reductive OTTLE studies of **2** in 0.1 M TBABF₄/DMF showing mono-reduced (left) and di-reduced (right) with applied potentials of -1.15 V and -1.4 V respectively (*vs.* Ag/AgCl). Mono-oxidised spectrum shown as dashed blue line in di-reduced graph for clarity.

Compound	Absorption / cm^{-1} ($\epsilon / \text{M}^{-1} \text{cm}^{-1} 10^3$)
[Pro-L] ⁺	38300 (14.0), 30050 (4.2), 22200 (10.7), 12230 (9.2)
[Pro-L] ²⁺	42650 (16.3), 38480 (15.2), 34024 (11.3), 14840 (19.4)
[Ru(bpy) ₂ L] ⁺	8980 (1.2), 12900 (1.2), 21880 (6.1), 29690 (13.6), 34200 (43.7)
[Ru(bpy) ₂ L] ²⁺	8980 (2.1), 12660 (2.4), 24200 (8.3), 34250 (41.7)
[Ru(decbpy) ₂ L] ⁺	9240 (5.1), 22540 (13.8), 31540 (49.4)
[Ru(decbpy) ₂ L] ²⁺	9190 (7.6), 12960 (4.9), 23880 (15.4), 31710 (47.8)
^b [Ru(decbpy) ₂ L] ³⁺	9170 (11.0), 14420 (7.2), 23720 (16.7), 32020 (46.4)
[Ru(decbpy) ₂ L] ⁻	6475 (2.9), 18470 (13.5), 19840 (14.9), 26780 (23.3), 31300 (45.8), 34830 (35.1)
[Ru(decbpy) ₂ L3] ²⁻	6170 (7.4), 18380 (15.5), 21000 (18.7), 28550 (36.5), 31450 (38.1), 34790 (39.5)

^b Study carried out in 0.3 M TBABF₄/DCM.

Table S1. Absorption spectra maxima of electrochemically mono-oxidised and di-oxidised (SC₂H₄CN)₂TTF(SMe)₂, mono-oxidised, di-oxidised, tri-oxidised, mono-reduced, di-reduced **2**, and mono-oxidised, di-oxidised and tri-oxidised **1**.

Hybrid DFT Calculations

The calculated optimised structure of **2** showed a 'kinked' TTF moiety with a torsion angle of 158.5° between C11-C13-S14-C15 (Fig. S10). Whilst a crystal structure was not obtained of this complex to verify if this is a true representation of the system, the structure can be compared to the 54 examples in the Cambridge Crystallographic Database³ of complexes where transition metals are directly bound to a TTF ligand. The majority of these structures are copper and nickel complexes, but there are also a number of platinum group metal complexes, namely platinum, palladium, iridium and one example of a rhodium structure. A comparison of the torsion angles on the TTF ligand for all monometallic structures in this search showed that all but three complexes had a torsion angle greater than 160° , those exceptions were two platinum and one gold complex. With examples of the 'kinked' TTF available it may be concluded that the calculated structure is a reliable representation of the system.

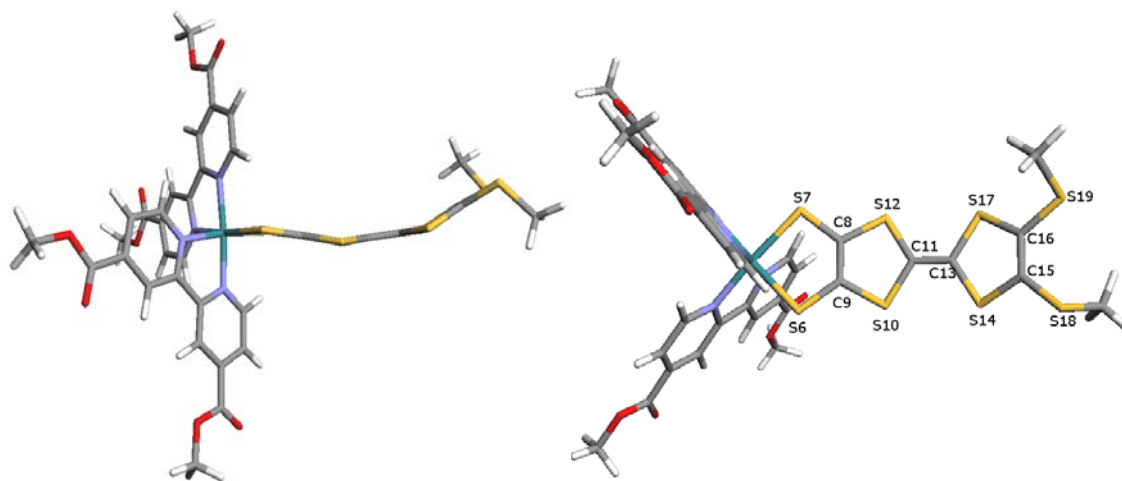


Figure S10. Optimised geometry of **2** in a DMF polarisable continuum model (left), with relevant atom labelling (right).

Molecular orbital	Energy (eV)	% Ru	% decbpy	% TTF
LUMO+1	-2.67	10.66	87.28	2.02
LUMO	-2.75	7.75	90.11	2.12
HOMO	-4.35	6.77	4.73	88.45
HOMO-1	-5.20	14.54	3.76	81.72
HOMO-2	-5.52	57.08	7.59	35.33

Table S2. Calculated energies and percentage contributions of Ru, decbpy, TTF for selected orbitals of **2** in DMF.

Excited state	Energy (nm)		f	Character
	Calculated	Observed		
2	1114	-	0.023	HOMO to LUMO (14%) LLCT (TTF-bpy)
				HOMO to LUMO+1 (80%) LLCT (TTF-bpy)
11	515	563	0.12	HOMO-3 to LUMO (74%) MLCT (Ru-bpy)
19	444	484	0.19	HOMO-4 to LUMO+1 (48%) MLCT (Ru-bpy)
27	385	400	0.14	HOMO-3 to LUMO+3 (66%) MLCT
33	362	400	0.14	HOMO to LUMO+9 (34%) LLCT (TTF-bpy)
				HOMO to LUMO+10 (31%) LLCT (TTF-bpy)
63	300	317	0.36	HOMO-10 to LUMO+1 (57%) bpy intraligand

Table S3. Summary of selected calculated excited state transitions, energies and character for **2** in DMF. Only those with oscillator strength greater than 0.1 are shown, with the exception of the HOMO-LUMO transition.

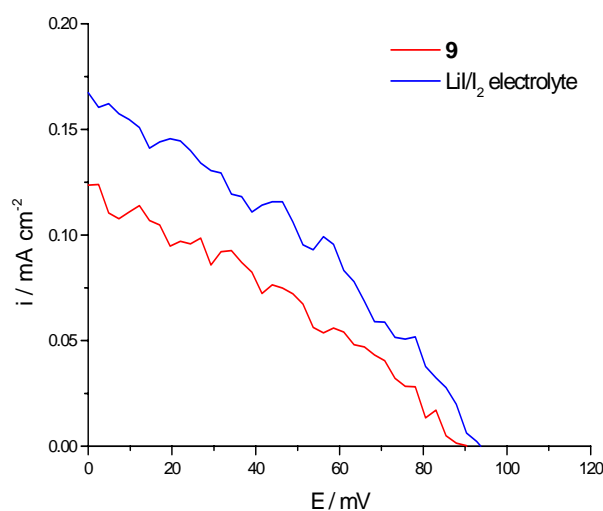


Figure S11. AM 1.5 (1000 Wm^{-2}) I-V characteristics for DSSCs sensitised with **3**.

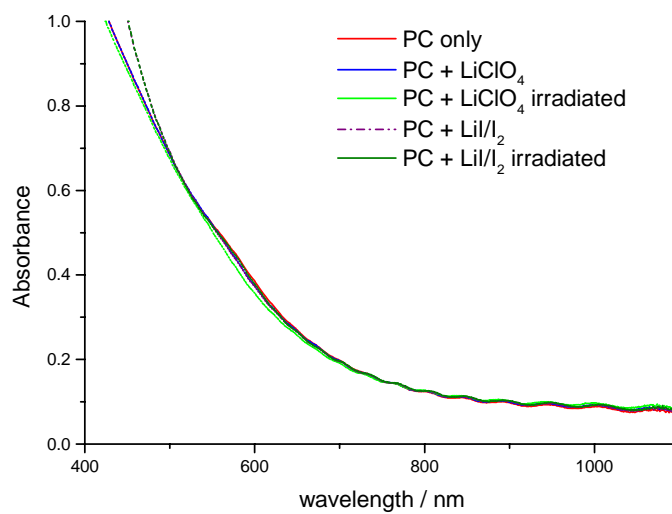


Figure S12. Absorption spectra of TiO₂ films sensitised with **3** with varying electrolytes, before and after TAS studies.

¹ D.L. Lichtenberger, R.L. Johnston, K. Hinkelmann, T. Suzuki, F. Wudl, *J. Am. Chem. Soc.*, 1990, **112**, 3302-3307.

² V. Gutmann, *Coord. Chem. Rev.*, 1967, **2**, 239.

³ D.A. Fletcher, R.F. McMeeking, D.J. Parkin, *J. Chem. Inf. Comput. Sci.*, 1996, **36**, 746-749.